JOURNAL OF CATALYSIS 109, 61–75 (1988)

Lanthana-Promoted Rh/SiO_2

I. Studies of CO and H_2 Adsorption and Desorption

RICHARD P. UNDERWOOD AND ALEXIS T. BELL

Materials and Molecular Research Division, Lawrence Berkeley Laboratory, and Department of Chemical Engineering, University of California, Berkeley, California 94720

Received January 6, 1987; revised August 4, 1987

Promotion of a Rh/SiO_2 catalyst with lanthana results in a partial coverage of the supported Rh crystallites with LaO_x islands. These moieties reduce the capacity of Rh to adsorb CO but have little effect on the chemisorption of H_2 because of spillover of H atoms from the exposed Rh sites onto the surface of the LaO_x islands. At elevated temperatures, the LaO_x islands promote the dissociation of CO. It is proposed that this process occurs preferentially at Rh sites located along the perimeter of the LaO_x islands. Support for this interpretation is provided by infrared spectra of CO adsorbed on lanthana-promoted Rh/SiO_2.

INTRODUCTION

Extensive studies of CO hydrogenation over Rh have established that catalyst activity and selectivity are strongly influenced by the composition of the Rh precursor (*1–3*), the size of the dispersed Rh particles (*4–6*), the support composition (*1, 7–14*), and, if a promoter is added, its composition (*15–27*). Because of the interactions of these four factors, it is often difficult to explain why different Rh catalysts exhibit different catalytic properties. Thus, for example, in a recent investigation of Rh/La_2O_3 catalysts (*6*), we established that with increasing Rh loading, not only did the size of the Rh particles increase, but also the extent to which the surface of the Rh particles was covered by LaO_x islands. Since both dispersion and LaO_x decoration are known to affect the catalytic properties of Group VIII metals for CO hydrogenation, the extent to which each of these factors contributed to the observed changes in the performance of Rh/La_2O_3 catalysts could not be ascertained. In order to understand more fully the specific effect of the LaO_x overlayer in the absence of changing Rh particle size, we have undertaken the present study of lanthana-promoted Rh/SiO_2 catalysts. The catalysts were characterized by H_2 and CO chemisorption measurements, temperature-programmed reduction (TPR), temperature-programmed desorption (TPD) of H_2 and CO, temperature-programmed surface reaction (TPSR) of adsorbed CO with H_2, and CO chemisorption combined with infrared spectroscopy as a probe of the catalyst surface structure. An investigation of the catalytic properties of these catalysts is reported separately (*28*).

EXPERIMENTAL

Catalyst Preparation

A large batch (30 g) of 4 wt% Rh/SiO_2 was prepared by incipient wetness impregnation of M-5 Cab-O-Sil (210 m^2/g, Cabot Corp.) with an aqueous solution of Rh $(NO_3)_3$–$2H_2O$ (Alpha Products). Following impregnation, the catalyst was dried at ambient temperature for 24 h and then in vacuum for 6 h at 333 K. The powder was pressed, crushed, and screened to 30–60 mesh size and calcined at 623 K in flowing 21% O_2/He for 2 h. Reduction was carried out at 623 K in flowing H_2 for 15 h. After

0021-9517/88 $3.00

reduction, the catalyst was flushed with He, cooled to ambient temperature, and passivated with air.

Portions of the reduced and passivated 4% Rh/SiO_2 catalyst were ground and then impregnated to incipient wetness with aqueous solutions of $La(NO_3)_3$ (Apache Chemicals). The concentration of $La(NO_3)_3$ in solution was adjusted to yield the desired La content. Following impregnation of Rh/SiO_2 with $La(NO_3)_3$ solution, the catalyst was dried at ambient temperature for 24 h, then dried in vacuum at 333 K for 6 h. The powder was again pressed, crushed, and screened to 30–60 mesh size, after which it was calcined at 623 K for 2 h. The promoted catalysts were reduced at 623 K for 15 h in flowing H_2, flushed with He, and then cooled and passivated.

Volumetric Chemisorption Measurements

The CO and H_2 chemisorption quantities were determined by means of a diffusion-pumped, volumetric adsorption apparatus equipped with an electronic manometer. Catalyst samples of approximately 0.6 g were reduced *in situ* at 573 K for 3 h, then evacuated at 573 K for 15 h prior to being cooled to the adsorption temperature. The total adsorbate uptake was determined by extrapolating the linear portion of the isotherm to zero pressure. The amount of reversible chemisorption was determined by evacuating the sample at 298 K for 30 min following determination of the total adsorbate uptake, and then measuring a second isotherm. The difference in the zero pressure intercepts for the two isotherms is defined as the amount of irreversible chemisorption.

Infrared Spectroscopy of Chemisorbed CO

The gas flow system and infrared cell have been described previously (*14*, *29*). A 0.05–0.10-g sample wafer of catalyst was reduced in the infrared cell at 563 K for 2 h. The sample was subsequently flushed with He at 563 K for 1 h and cooled in flowing He to 313 K, after which a reference spectrum was taken. The sample was then exposed to 100 Torr CO in He for 30 min followed by a 10 min He flush before the sample spectrum was recorded. Spectra were recorded at 8 cm^{-1} resolution by means of a Digilab FTS 15/80 dual-beam FTIR spectrometer equipped with a narrow-band MCT detector.

TPR, TPD, and TPSR

The apparatus used for the temperature-programmed experiments has been described previously (*30*). The procedure for conducting such experiments is as follows. A catalyst sample was placed in a quartz microreactor which could be heated at up to 1 K/s. For all samples, the quantity of surface Rh atoms (based on the unpromoted catalyst) in the microreactor was kept at approximately 3.8×10^{-6} mol. The desorbing gas was swept from the microreactor by a continuous flow of carrier gas. Analysis of the effluent flow was performed with a quadrupole mass spectrometer. A microcomputer was used to direct the mass spectrometer to a series of preselected masses and to record the signal intensity at each mass setting. In addition to the mass signal intensities, the temperature was also recorded by the microcomputer.

Prior to a TPR measurement, the sample was calcined at 623 K for 1.5 h, then cooled to 293 K and evacuated for 10 min. A mixture of 970 ppm H_2 in He was fed to the reactor at 150 cm^3/min and the temperature was ramped linearly at 0.25 K/s while the H_2 consumption was monitored.

TPD experiments were initiated by reducing the sample at 573 K for 2 h in H_2 flowing at 100 cm^3/min. After reduction, the sample was evacuated and the temperature was increased linearly at 0.25 K/s to 873 K. The temperature was held at 873 K in vacuum for 10 min before being lowered to the adsorption temperature of 293 K. This procedure was necessary in order to ensure desorption of all of the H_2 so that a flat baseline could be obtained during TPD.

TABLE 1

Lanthanum Content of Lanthana-Promoted Rh/SiO_2 Catalysts

Catalyst	La/Rh_s[a]	wt% La_2O_3
Rh/SiO_2	0	0
$La(0.1)/Rh/SiO_2$	0.1	0.25
$La(0.5)/Rh/SiO_2$	0.5	1.18
$La(1.0)/Rh/SiO_2$	1.0	2.46
$La(2.5)/Rh/SiO_2$	2.5	5.59
$La(5.0)/Rh/SiO_2$	5.0	10.6
$La(10.0)/Rh/SiO_2$	10.0	18.7

[a] See text for explanation of La/Rh_s.

Saturation adsorption was achieved by flowing or pulsing pure CO or H_2 over the sample, followed by evacuation for 5 min at 293 K. The flow was then switched to 50 cm^3/min of He carrier and the temperature was ramped linearly at 1 K/s to 873 K (H_2 TPD) or 923 K (CO TPD) while desorption products were monitored.

Sample pretreatment prior to TPSR measurements was the same as for TPD. CO was adsorbed by pulsing pure CO (several monolayer equivalents) at either 298 or 673 K. The sample was then cooled to 293 K, and subsequently heated at 1 K/s from 293 to 783 K in 50 cm^3/min of pure H_2.

High-purity He carrier gas was further purified by passage through an oxygen adsorbent (Oxysorb, Alltech) and a packed tube of molecular sieve cooled to 77 K. Ultrahigh-purity H_2 (Matheson) was further purified by passage through a catalytic purifier (Engelhard) and a molecular sieve trap cooled to 77 K. Ultrahigh-purity CO (Matheson) was purified by passage through a molecular sieve trap maintained at ambient temperature, and $C^{18}O$ (98%, Liquid Carbonic) was used without further purification.

RESULTS

Catalyst Characterization

Table 1 identifies the catalysts used in this investigation. The middle column lists the quantities of La added to the Rh/SiO_2 catalyst expressed as La/Rh_s. The concentration of surface Rh atoms was determined by irreversible H_2 chemisorption at 298 K on the unpromoted Rh/SiO_2 catalyst, assuming an H_s to Rh_s stoichiometry of 1 : 1. It should be emphasized that La/Rh_s is not indicative of the quantity of La on the surface of the Rh crystallites since some of the added La may reside on the surface of the SiO_2. The third column of Table 1 shows the calculated weight loading of La_2O_3, assuming that the lanthanum exists in that form.

Table 2 shows the influence of lanthana content on H_2 chemisorption at 195 and 298 K and on CO chemisorption at 298 K. The

TABLE 2

Influence of La Content on H_2 and CO Chemisorption

La/Rh_s	T_{ads} = 195 K		T_{ads} = 298 K		T_{ads} = 298 K	
	H_t/Rh[a]	H_{irr}/Rh[b]	H_t/Rh[a]	H_{irr}/Rh[b]	CO_t/Rh[a]	CO_{irr}/Rh[b]
0	0.64	0.54	0.64	0.38	0.50	0.43
0.1	0.61	0.49	0.55	0.33	0.50	0.44
0.5	0.60	0.47	0.56	0.34	0.48	0.43
1.0	0.43	0.32	0.44	0.24	0.35	0.32
2.5	0.56	0.43	0.52	0.32	0.30	0.26
5.0	0.49	0.39	0.50	0.31	0.20	0.16
10.0	0.43	0.34	0.50	0.34	0.15	0.10

[a] Total chemisorption, irreversible plus reversible (see text for explanation).
[b] Irreversible chemisorption.

quantities H_t/Rh and H_{irr}/Rh appearing in Table 2 are defined as the ratios of total H adsorbed and irreversible H adsorbed, respectively, to the total Rh in the catalyst. CO_t/Rh and CO_{irr}/Rh are defined as the ratios of total CO adsorbed and irreversible CO adsorbed, respectively, to the total Rh in the catalyst.

With the possible exception of La(10)/Rh/SiO_2, H_t/Rh measured at 195 K agrees reasonably well with H_t/Rh measured at 298 K for each catalyst. A monotonic decrease in H_t/Rh with increasing weight loading is observed. The values of H_{irr}/Rh measured at 195 K and of CO_{irr}/Rh measured at 298 K both decrease with increasing lanthana content, but the extent of the decrease is not the same. H_{irr}/Rh (195 K) decreases from 0.54 for Rh/SiO_2 to 0.34 for La(10)/Rh/SiO_2, while CO_{irr}/Rh decreases from 0.43 to 0.10 for Rh/SiO_2 and La(10)/Rh/SiO_2, respectively. By contrast, H_{irr}/Rh measured at 298 K is relatively constant as the lanthanum content increases.

The values of H_t/Rh and H_{irr}/Rh given in Table 2 for La(1.0)/Rh/SiO_2 are slightly lower than expected when compared with the values observed for La(0.5)/Rh/SiO_2 and La(2.5)/Rh/SiO_2. The lower than expected chemisorption values for the La(1.0)/Rh/SiO_2 catalyst cannot be attributed to sintering of the Rh particles in this sample since, as noted below, the Rh dispersion for all seven of the catalysts was virtually the same.

All of the samples were examined by X-ray diffraction. Within experimental accuracy, the shape and width of the Rh(111) peak were the same for every sample. The Rh particle size calculated from line broadening was 3.3 nm. This value is in good agreement with the 3.5 nm calculated from H_{irr}/Rh (298 K) for Rh/SiO_2 on the assumption that Rh particles are hemispherical. These results indicate that, within the experimental accuracy of the measurements, the Rh particle size is unaffected by the addition of lanthana.

Infrared Spectroscopy of Chemisorbed CO

Figure 1 shows the influence of lanthana content on the infrared spectrum of CO chemisorbed at 313 K. The absorbance is normalized to the quantity of surface Rh atoms, measured by H_2 chemisorption at 298 K, for the unpromoted Rh/SiO_2 catalyst.

The spectrum for Rh/SiO_2 (spectrum A in Fig. 1) shows three main features. The most intense band, at 2064 cm^{-1}, corresponds to linearly adsorbed CO. This band is flanked by weak shoulders on either side corresponding to the symmetric and asymmetric stretching vibrations of the *gem*-dicarbonyl, $Rh(CO)_2$. The broad feature, with a peak maximum at 1905 cm^{-1}, corresponds to bridge-adsorbed CO and appears to be composed of two overlapping bands, due probably to bridging CO coordinated to different Rh crystal faces. Unfortunately, insufficient single-crystal data are available

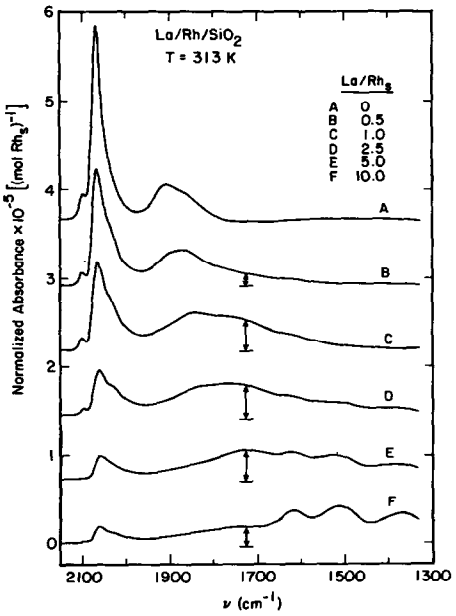

FIG. 1. The influence of La content on the infrared spectrum of chemisorbed CO. Absorbance has been normalized to the concentration of surface Rh atoms in the unpromoted Rh/SiO_2 catalyst. The double arrow indicates the intensity of the band at 1725 cm^{-1}.

to assign each band to a specific form of bridging CO.

The influence of lanthana content on the spectra is rather dramatic, and the degree of perturbation of the spectrum from that observed for Rh/SiO_2 increases with increasing lanthana content. It is apparent that the band for linearly adsorbed CO decreases dramatically with lanthana content. Though it is difficult to separate accurately the bands for the dicarbonyl species from the band for linearly adsorbed CO, deconvolution indicates that the amount of linearly adsorbed CO for $La(10)/Rh/SiO_2$ is only 14% of that for Rh/SiO_2. The frequency of the band for linearly adsorbed CO, which is sensitive to CO coverage because of vibrational coupling of adjacent CO dipoles (31), shifts from 2064 cm^{-1} for Rh/SiO_2 to 2056 cm^{-1} for $La(10)/Rh/SiO_2$. The bands for $Rh(CO)_2$ and bridging CO also decrease with lanthana content, though the decrease in the bands for $Rh(CO)_2$ is not as great as for linearly adsorbed CO.

Figure 1 shows that an additional effect of lanthana promotion is to give rise to new bands in the region below 1800 cm^{-1}. These features, which are seen more clearly in Fig. 2, occur at 1725, 1620, 1520, and 1370 cm^{-1}. It is clear from Fig. 1 that the bands at 1620, 1520, and 1370 cm^{-1} increase monotonically with lanthana content. The band at 1725 cm^{-1}, however, increases with lanthana content up to La/Rh_s of about 2.5–5.0 and then decreases for $La(10)/Rh/SiO_2$. Assignment of these bands will be discussed later.

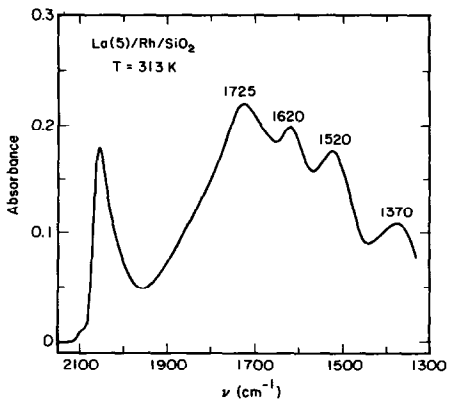

FIG. 2. The infrared spectrum of chemisorbed CO on $La(5)/Rh/SiO_2$ (spectrum E from Figure 2).

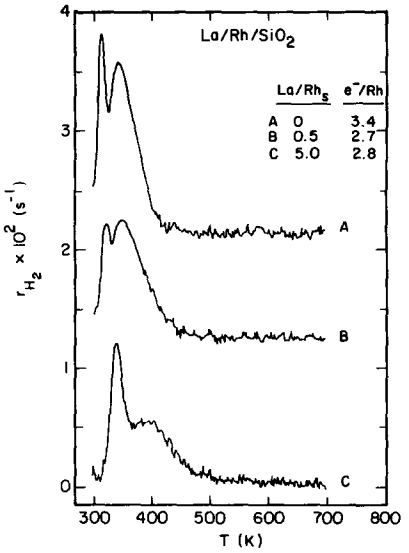

FIG. 3. Temperature-programmed reduction (TPR) spectra for Rh/SiO_2, $La(0.5)/Rh/SiO_2$, and $La(5)/Rh/SiO_2$.

Temperature-Programmed Reduction

TPR spectra obtained for Rh/SiO_2, $La(0.5)/Rh/SiO_2$, and $La(5)/Rh/SiO_2$ are presented in Fig. 3. Also shown is the extent of reduction of Rh, calculated from the H_2 consumption, expressed as the number of electrons per Rh atom. Reduction of Rh_2O_3 to Rh^0 requires $3e^-/Rh$, and, as can be seen, the values of e^-/Rh values are within approximately 10% of 3.0 for all three catalysts. The estimated experimental accuracy in the determination of e^-/Rh is approximately $\pm 10\%$.

The TPR spectra for all three catalysts are composed of two peaks, a sharp peak followed by a broader peak. The positions of both peaks shift to higher temperature with increasing lanthana content. Lanthana addition also affects the relative sizes of the two peaks.

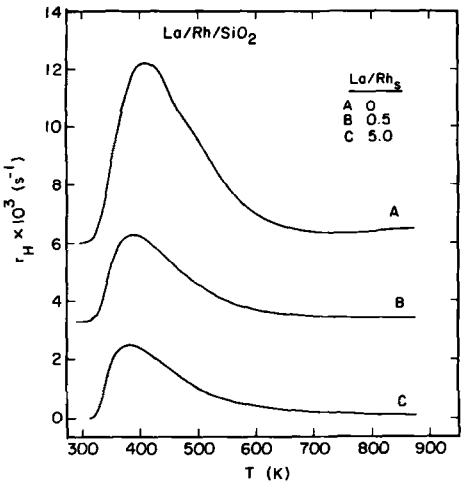

FIG. 4. Desorption of H_2 from Rh/SiO_2, La(0.5)/Rh/SiO_2, and La(5)/Rh/SiO_2.

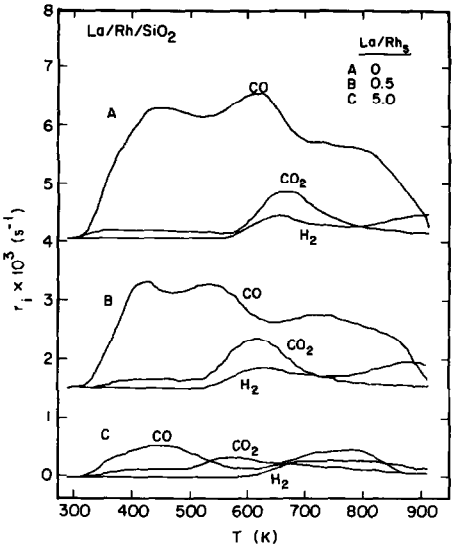

FIG. 5. Desorption of CO from Rh/SiO_2, La(0.5)/Rh/SiO_2, and La(5)/Rh/SiO_2.

Temperature-Programmed Desorption of H_2 and CO

The results for TPD of H_2 and CO are shown in Figs. 4 and 5, respectively. Each of the spectra shown are for saturation coverage by H_2 or CO. Presented in Table 3 are the quantities of desorbed H, CO, and CO_2 obtained by integration of the TPD spectra.

As can be seen in Fig. 4, the lanthana content has little influence on the shape of the H_2 desorption spectrum. The TPD spectra for all three catalysts show one peak, and the peak temperature decreases with lanthana content from 405 K for Rh/SiO_2 to 385 K for La(5)/Rh/SiO_2. Only for Rh/SiO_2 does the quantity of H_2 desorbed, given in Table 3, agree with that expected on the basis of the volumetric chemisorption results (Table 2). The values for H_{irr}/Rh measured at 298 K from Table 2 predict that 3.82×10^{-6}, 3.47×10^{-6}, and 3.15×10^{-6} mol of H would have desorbed from Rh/SiO_2, La(0.5)/Rh/SiO_2, and La(5)/Rh/SiO_2, respectively. The values of 1.88×10^{-6} and 1.66×10^{-6} mol obtained from integration of the TPD spectra for La(0.5)/Rh/SiO_2 and La(5)/Rh/SiO_2, respectively, are roughly half of those obtained from chemisorption measurements. The reason for this difference is unclear. One possibility is that after evacuation of the catalyst at

TABLE 3

Quantities of H, CO_2, and CO Desorbed during TPD

Catalyst	Rh_s[a] (mol)	H_2 TPD	CO TPD				
		H (mol)	CO (mol)	CO_2 (mol)	H (mol)	C_s[b] (mol)	CO_t[c] (mol)
Rh/SiO_2	3.82×10^{-6}	4.06×10^{-6}	4.02×10^{-6}	0.55×10^{-6}	0.39×10^{-6}	0.16×10^{-6}	4.73×10^{-6}
La(0.5)/Rh/SiO_2	3.88×10^{-6}	1.88×10^{-6}	2.90×10^{-6}	0.60×10^{-6}	0.49×10^{-6}	0.11×10^{-6}	3.61×10^{-6}
La(5)/Rh/SiO_2	3.86×10^{-6}	1.66×10^{-6}	0.70×10^{-6}	0.31×10^{-6}	0.24×10^{-6}	0.07×10^{-6}	1.08×10^{-6}

[a] Based on H chemisorption at 298 K on Rh/SiO_2 before promotion with La.
[b] Based on the moles of CO_2 desorbed minus the moles of H desorbed.
[c] Based on the moles of CO plus twice the moles of CO_2 minus the moles of H desorbed.

873 K, before a TPD spectrum is obtained, the surface structure of the catalyst is different from that present after evacuation at 573 K, the temperature used for the chemisorption measurements. Since, for Rh/SiO_2, the quantity of H_2 desorbed during TPD is in close agreement with volumetric chemisorption, it is unlikely that the diminished capacity for H_2 chemisorption on the lanthana-promoted TPD samples is a result of sintering of the Rh particles.

The CO TPD results, shown in Fig. 5, indicate that the lanthana content has a large influence on the CO binding states. The CO desorption spectrum is composed of several peaks, indicating the existence several binding states. The presence of lanthana decreases CO adsorption on all sites and preferentially on sites of intermediate binding energy, that is, those desorbing at about 600 K.

As shown in the Fig. 5, CO desorption is accompanied by the production of CO_2 and H_2 for all three catalysts. CO_2 is produced in two peaks, a broad low-temperature peak below 500 K followed by a larger peak above 500 K. The peak temperature of the second peak decreases with lanthana content from 670 K for Rh/SiO_2 to 570 K for $La(5)/Rh/SiO_2$. H_2 is produced in two peaks during CO TPD on Rh/SiO_2 and $La(0.5)/Rh/SiO_2$ and in one broad peak on $La(5)/Rh/SiO_2$. The first H_2 peak is coincident with the CO_2 peak for Rh/SiO_2 and $La(0.5)/Rh/SiO_2$.

CO_2 can be produced during CO TPD by both the disproportionation of CO,

$$2CO_s \rightarrow CO_2 + C_s, \qquad (1)$$

and by the reaction of CO with hydroxyl groups from the support or promoter,

$$CO_s + OH_s \rightleftarrows CO_2 + \tfrac{1}{2}H_2. \qquad (2)$$

The observed production of H_2 during CO TPD and the results of isotope labeling studies, presented below, indicate that a portion of the CO_2 formed during CO TPD is produced by the reaction of CO with hydroxyl groups.

The quantity of surface carbon, C_s, produced by CO disproportionation can be determined from the difference between the quantities of CO_2 and H_2 desorbed. Table 3 indicates the amount of surface carbon deposited on each catalyst. The quantity of CO adsorbed prior to TPD is therefore equal to (moles of CO desorbed) + 2(moles of CO_2 produced) − (moles of H produced). This quantity is listed in the last column of Table 3. It is evident from the last two columns of Table 3 that the quantity of surface carbon deposited by disproportionation, relative to the CO chemisorption capacity of each catalyst, increases with La content.

In order to investigate the production of CO_2 during CO TPD in more detail, experiments using $C^{18}O$ were performed. Figures 6, 7, and 8 show the desorption products obtained during TPD of $C^{18}O$ on Rh/SiO_2, $La(0.5)/Rh/SiO_2$, and $La(5)/Rh/SiO_2$, respectively. Both ^{18}O-labeled and unlabeled CO and CO_2 were monitored during the temperature ramp. Since the He carrier gas used was of extremely high purity, the only sources of ^{16}O in these experiments were the small $C^{16}O$ impurity

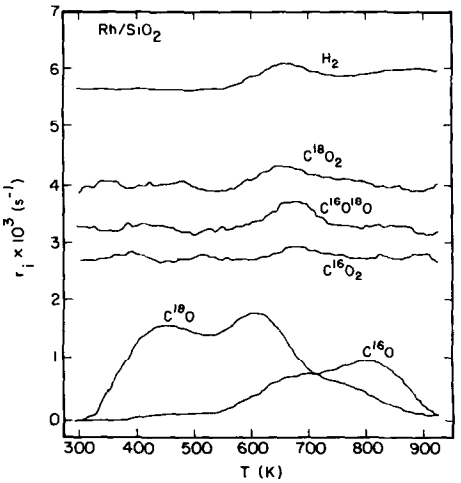

FIG. 6. Product desorption rates during $C^{18}O$ desorption from Rh/SiO_2.

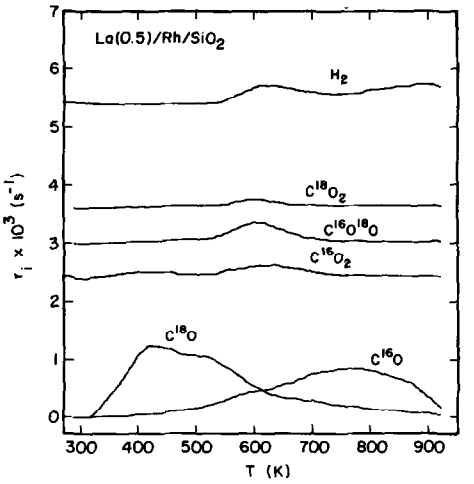

FIG. 7. Product desorption rates during $C^{18}O$ desorption from La(0.5)/Rh/SiO_2.

in the $C^{18}O$ (approx. 2%) and ^{16}O from the catalyst.

As can be seen in Fig. 6 for Rh/SiO_2, a large quantity of ^{16}O was observed in both the CO and CO_2. The observed amounts of CO and CO_2 containing ^{16}O were much greater than that which can be attributed to the ^{16}O impurity in the $C^{18}O$. Most of the CO_2 molecules produced contain at least one ^{16}O atom and, above 705 K, most of the CO desorbs as $C^{16}O$. Production of $C^{16}O$ begins at temperatures as low as 380 K, but the rate increases dramatically at about 550 K, coincident with the start of the second peak for the production of CO_2. Figures 7 and 8 show that the extent of ^{18}O-labeling in CO and CO_2 decreases with increasing lanthana content. For La(5)/Rh/SiO_2, virtually all of the CO_2 produced is $C^{16}O_2$.

Temperature-Programmed Surface Reaction

Figure 9 shows the TPSR spectra of CO adsorbed at 298 K for Rh/SiO_2, La(0.5)/Rh/SiO_2, and La(5)/Rh/SiO_2. For each catalyst the quantity of CH_4 produced is in good agreement with the quantity of CO adsorbed prior to the TPD measurements (last column of Table 3). The small spike at the beginning of each spectrum is attributed to a perturbation in the mass spectrometer signal caused by switching the microreactor feed from He to H_2, since the same spike was seen when the feed was switched from He to H_2 through a blank reactor. The perturbation occurs because the method of

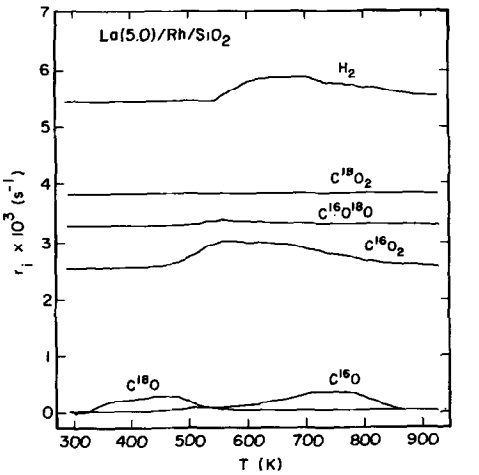

FIG. 8. Product desorption rates during $C^{18}O$ desorption from La(5)/Rh/SiO_2.

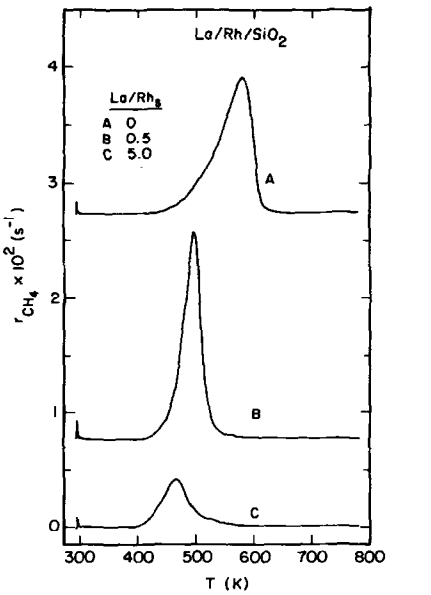

FIG. 9. Hydrogenation of CO preadsorbed at 298 K on Rh/SiO_2, La(0.5)/Rh/SiO_2, and La(5)/Rh/SiO_2.

data processing is such that the CH_4 signal is recorded by dividing the $m/e = 15$ signal for CH_4 by the $m/e = 2$ signal for H_2. Since the response of the background signal for each mass to the switch from He to H_2 is not exactly the same, the result is an excursion in the recorded signal.

As can be seen in Fig. 9, a single CH_4 peak is observed for all three catalysts and the peak temperature shifts downscale from 585 K for Rh/SiO_2 to 470 K for $La(5)/Rh/SiO_2$. The increased reactivity of CO when Rh/SiO_2 is promoted with lanthana is consistent with the increased steady-state CO hydrogenation activity observed for the lanthana-promoted catalysts described in the second part of this study (*28*). The greater initial slopes of the TPSR peaks for the lanthana-promoted samples compared with that for Rh/SiO_2 is consistent with the observation that the activation energy for the production of CH_4 is higher on the lanthana-promoted Rh/SiO_2 (*28*).

In order to detect the possible formation of surface carbon formed by CO dissociation and the influence of lanthana promoter on this reaction, TPSR spectra were recorded after CO was preadsorbed at an elevated temperature. Figure 10 shows the influence of lanthana content on the TPSR spectrum of CO preadsorbed at 673 K. In these experiments, five pulses of pure CO (several monolayer equivalents) were passed through the catalysts by injection into the carrier stream at 673 K. Following the CO pulses, the temperature was held at 673 K for 10 min prior to being lowered to the ambient temperature. As can be seen in Fig. 10, CH_4 was produced immediately upon exposure to H_2 for all three catalysts. Higher-temperature CH_4 peaks, similar to those observed for CO adsorption at 298 K in Fig. 9, are also observed but are of much lower intensity because most of the CO desorbs after 10 min at 673 K.

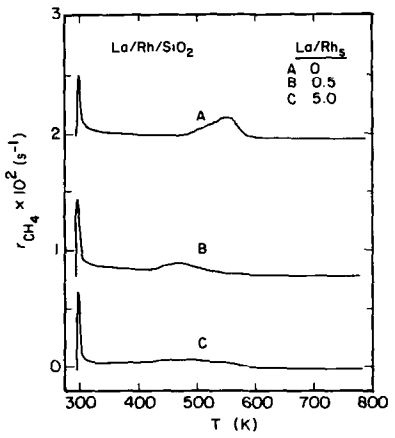

FIG. 10. Hydrogenation of CO preadsorbed at 673 K on Rh/SiO_2, $La(0.5)/Rh/SiO_2$, and $La(5)/Rh/SiO_2$.

The source of the CH_4 formed immediately upon exposure to H_2 is presumed to be surface carbon produced by CO dissociation during adsorption at 673 K. It is clear that the amount of surface carbon formed, relative to the CO chemisorption capacity of each catalyst, increases with lanthana content. The quantities of surface carbon formed, obtained from integration of the first CH_4 peak and expressed as the fraction of the CO chemisorption capacity, are 0.08, 0.13, and 0.36 for Rh/SiO_2, $La(0.5)/Rh/SiO_2$, and $La(5)/Rh/SiO_2$, respectively.

DISCUSSION

Catalyst Structure and Composition

Information regarding the physical state of the catalysts is provided by XRD and TPR. From the width of the Rh(111) peak in the XRD pattern of reduced Rh/SiO_2, the diameter of the average Rh crystallite is determined to be 3.3 nm. The shape and width of the Rh(111) peak of the lanthana-promoted catalysts are the same as those for the original Rh/SiO_2 catalyst, indicating that, within the experimental accuracy of the XRD measurements, lanthana promotion does not alter the Rh particle size. XRD peaks for La_2O_3 were observed only for the catalysts of highest lanthana content. These peaks are very broad and diffuse, indicating that the diameter of the observed La_2O_3 crystal domain is less than 4 nm.

The location of the lanthana promoter relative to the supported Rh particles cannot be established directly and so must be inferred. As is discussed below, the observation that the CO chemisorption capacity of the catalyst declines with increasing level of promotion suggests that at least a portion of the promoter resides on the surface of the Rh particles, possibly in the form of LaO_x patches. Such a model is identical to that used previously by Rieck and Bell (*33*) to interpret the effects of rare-earth oxide promoters on the chemisorptive and catalytic properties of Pd/SiO_2 and by Hicks *et al.* (*34*) to interpret the chemisorptive properties of Pd/La_2O_3.

The TPR results for Rh/SiO_2, $La(0.5)/Rh/SiO_2$, and $La(5)/Rh/SiO_2$ indicate that, within the estimated 10% experimental accuracy of the measurements, the consumption of H_2 for all three catalysts corresponds to a $3e^-/Rh$ reduction of Rh_2O_3 to Rh^0. Though the origins of the two peaks observed in the TPR spectra are uncertain, it is possible that the first peak corresponds to the rapid reduction of surface Rh while the second peak corresponds to the slower reduction of Rh_2O_3 in the interior of the Rh_2O_3 particles. The shift of both the first and second peaks to higher temperature with increasing lanthana content may be due to lanthanum oxide on the surface of the particles. Surface lanthanum oxide blocks part of the surface, making the adsorption of H_2 and subsequent reduction of Rh_2O_3 more difficult. It is also possible that some surface lanthanum rhodate ($LaRhO_3$) is formed during calcination of the catalysts. Such a surface perovskite phase would be expected to reduce at a higher temperature than does Rh_2O_3 (*32*).

The above discussion does not consider the possible reduction of La_2O_3 to LaO_x ($x = 1.5$), a process which has been observed for lanthana-promoted Pd/SiO_2 (*33*). Since the TPR results of Fig. 4 give no indication of a separate peak corresponding to the reduction of La_2O_3, it is impossible to say whether any of the promoter in the lanthana-promoted Rh/SiO_2 catalysts undergoes reduction.

Interaction of H_2 and CO with Rh/SiO_2 and La-promoted Rh/SiO_2

The data presented in Table 2 indicate a decline in the CO chemisorption capacity of Rh/SiO_2 as it is promoted with progressively larger quantities of lanthana. A similar trend can also be deduced from the infrared spectra of adsorbed CO shown in Fig. 1. Since the size of the Rh particles remains unchanged as a consequence of lanthana promotion, we propose that the decrease in CO adsorption capacity is due to a partial coverage of the Rh particles by LaO_x. As is discussed below, infrared spectroscopy suggests that while a small amount of CO adsorbs on the promoter, the majority of the adsorbate is associated with Rh sites.

The effects of lanthana promotion on H_2 chemisorption are different from those observed for CO chemisorption. The data in Table 2 demonstrate that at both 195 and 298 K the decrease in H_2 adsorption capacity with increasing level of lanthana promotion is smaller than that observed for CO. It seems safe to assume that all of the chemisorbed H_2 is associated with the Rh particles, since recent studies conducted in this laboratory (*6*) have demonstrated the absence of H_2 spillover onto SiO_2 for adsorption temperatures between 195 and 298 K.

Careful comparison of the data for H_{irr}/Rh measured at 195 K and CO_{irr}/Rh measured at 298 K show the following patterns. For values of $La/RH_s = 0$ to 1.0, the values of H_{irr}/Rh and CO_{irr}/Rh are nearly the same, but for $La/Rh_2 \geq 2.5$ the value of H_{irr}/Rh exceeds the value of CO_{irr}/Rh. Our interpretation of this pattern is that at values of La/Rh_s below 2.0, H_2 chemisorbs exclusively on Rh sites not covered by LaO_x patches. At higher loadings of lanthana, though, a portion of the H_2 chemisorbed onto the Rh spills over onto the LaO_x patches. It is for this reason, we

believe, that H_{irr}/Rh exceeds CO_{irr}/Rh when $La/Rh_s \approx 2.0$. These results suggest, therefore, that caution must be used in applying H_2 chemisorption to determine either the dispersion of lanthana-supported metal or the extent to which supported particles are covered by oxide patches.

The TPD spectra for H_2, presented in Fig. 4, show no new features when Rh/SiO_2 is promoted with lanthana. This observation agrees very well with that of Rieck and Bell (*33*) for lanthana-promoted Pd/SiO_2. In further agreement is the observation that the amount of H_2 desorbed decreases upon lanthana promotion. The similarity of the H_2 spectra with and without promotion suggests that the observed desorption is from exposed Rh atoms. Likewise the suppression of H_2 adsorption with increasing lanthana promotion indicates that none of the adsorbed H_2 is present on the LaO_x patches covering the Rh particles. The reason why H_2 spillover onto the LaO_x patches was observed in the chemisorption experiments but not in the TPD experiments is unclear. One possibility is that the higher evacuation temperature used prior to the TPD experiments may change the structure of the LaO_x overlayer and render H spillover onto it more difficult.

Further insights into the chemisorption of CO on lanthana-promoted Rh/SiO_2 can be drawn from the results of infrared spectroscopy and temperature-programmed desorption spectroscopy. To proceed with this analysis, it is first necessary to discuss the assignment of the bands which appear below 1800 cm^{-1} in Figs. 1 and 2.

The bands at 1620, 1520, and 1370 cm^{-1} increase in rough proportion to the lanthana content of the catalyst. It is therefore reasonable to assign these bands to species formed by the reaction of CO with LaO_x. The bands at 1520 and 1370 cm^{-1} can be assigned to the asymmetric and symmetric vibrations of unidentate carbonate groups. The positions of these features are in reasonable agreement with those observed at 1500 and 1390 cm^{-1} by Rosynek and Magnuson (*35*) for CO_2 adsorption on La_2O_3.

The identity of the species giving rise to the band at 1620 cm^{-1} is unclear. Rosynek and Magnuson (*35*) observed bands at 1310 and 1565 cm^{-1} for CO_2 adsorbed on La_2O_3. They attributed these bands to the symmetric and asymmetric stretching vibrations of bidentate carbonate. If their assignment is correct, it seems unlikely that the band at 1620 cm^{-1} observed here corresponds to bidentate carbonate groups. It is also possible, however, that this band is due to bridging carbonate groups (*36*). Assignment of the 1620 cm^{-1} band to a formate species seems less likely, since such structures exhibit a band at 1585 cm^{-1} (*36*). While not observed here, evidence for formate groups was obtained when a lanthana-promoted Rh/SiO_2 catalyst was exposed to H_2 and CO at 530 K (*28*).

We postulate that the band at 1725 cm^{-1} corresponds to the stretching vibration of CO chemisorbed on Rh sites near the perimeter of LaO_x islands. The CO molecule may be envisioned as bonded to the Rh through the carbon end of the molecule and to a lanthanum cation through the oxygen end of the molecule. This type of bonding reduces the order of the C–O bond and lowers its vibrational frequency. Precedence for such bonding exists in the field of organometallic chemistry (*37, 38*), where it has been observed that coordination of the oxygen end of a carbonyl group to an electron acceptor (e.g., $AlCl_3$) results in a reduction of the C–O vibrational frequency. Similar forms of adsorbed CO have also been reported in other studies of supported Rh promoted with metal oxides. For example, Kiennemann *et al.* (*27*) observed an infrared band at 1725 cm^{-1} in their study of ceria-promoted Rh/SiO_2 catalysts, and Ichikawa and Fukushima (*39*) observed a band between 1600 and 1800 cm^{-1} when Rh/SiO_2 was promoted with titania, manganese oxide, and iron oxide. In both cases, the authors assigned the band below 1800 cm^{-1} to CO adsorbed near promoter cations

and interacting with both Rh and cationic sites.

Having considered the assignment of the low-frequency CO bands, we can return to a discussion of the influence of lanthana promotion on CO chemisorption. As can be seen in Table 2, CO_{irr}/Rh is constant with increasing lanthana content up to La/Rh_s = 0.5, and thereafter decreases dramatically with further increases in lanthana content. The infrared spectra of Fig. 1 show that with increasing lanthana content the amounts of linearly adsorbed CO and bridge-adsorbed CO decrease and the amount of CO adsorbed as carbonate increases. The presence of carbonate groups indicates that the values of CO_{irr}/Rh given in Table 2 reflect both adsorption on uncovered Rh and reaction with the LaO_x patches. The measured values of CO_{irr}/Rh must therefore be viewed as upper limits to the CO chemisorption capacity of the exposed surface Rh. Since the values of CO_{irr}/Rh decrease significantly while the values of H_{irr}/Rh (298 K) are nearly constant with increasing lanthana content, it is clear that the capacity of the LaO_x patches for CO is much less than that for H_2.

As mentioned earlier, the intensity of the band at 1725 cm^{-1} for CO interacting with lanthana cations increases with increasing lanthana content up to a La/Rh_s ratio of 2.5–5.0 and then decreases for La/Rh_s = 10. The occurrence of a maximum is consistent with the proposed assignment of this band to CO adsorbed near the perimeter of LaO_x patches. Since the initial addition of lanthana to the Rh surface results in the nucleation and growth of LaO_x patches, the concentration of surface Rh atoms along the perimeter of these patches initially increases with lanthana content. As the lanthana content is increased further, the LaO_x patches increase in size and eventually overlap, resulting in a decrease in total perimeter with further lanthana addition.

The TPD spectra for CO provide further information regarding the influence of lanthana on the interactions of CO with the catalyst surface. As may be seen in Fig. 5 and Table 3, lanthana promotion causes a suppression in the total amount of CO adsorbed. This trend parallels that observed in CO chemisorption, but the quantities of adsorbed CO on the lanthana-promoted samples determined from TPD spectra are somewhat smaller than those determined from chemisorption measurements. This discrepancy may be due to the lower adsorption time used for the TPD experiments or to changes in the structure of the LaO_x overlayer induced by the high evacuation temperature used prior to the TPD experiments.

The addition of lanthana also changes the appearance of the CO TPD spectrum. As the lanthana content of the catalyst increases, the intensity of the CO signal in the region from 500 to 600 K decreases, a pattern similar to that observed by Rieck and Bell (*33*) for lanthana-promoted Pd/SiO_2. Care must be taken in ascribing all of this change to modifications in the adsorptive properties of Rh by lanthana promotion since the decrease in CO signal intensity is accompanied by an increase in the intensity of the CO_2 signal. What this indicates is that a large part of the change in the CO signal is due to the enhanced formation of CO_2 effected by the promoter.

As noted earlier, CO_2 can be formed during the desorption of CO by CO disproportionation and the reaction of CO with hydroxyl groups from the support or promoter. The stoichiometries for these two reactions are as follows:

$$2CO_s \rightarrow CO_2 + C_s \qquad (1)$$

$$CO_s + OH_s \rightleftarrows CO_2 + \tfrac{1}{2}H_2 \qquad (2)$$

The occurrence of reaction 2 is well documented by the concurrent appearance of H_2 and CO_2 and by the isotopic labeling experiments presented in Figs. 6–8. The occurrence of reaction 2 was also proposed by Jackson (*40*) to explain the results of isotopic labeling experiments conducted with

SiO_2- and MgO-supported Rh. Not all of the CO_2 can be ascribed to reaction 2, though, since as shown by the data in Table 3, the amount of CO_2 produced always exceeds the amount of H_2. The difference in the amounts of CO_2 and H_2 formed is attributed to the occurrence of reaction 1. It is of interest to note that while the proportion of CO converted to CO_2 increases with lanthana addition, the results in Table 3 indicate that relative importance of reactions 1 and 2 is essentially independent of promoter level. Thus, it appears that lanthana promotes both reactions to an equivalent extent. Further evidence of the positive effect of lanthana promotion is the downscale shift in the temperature at which the maximum rate of CO_2 formation is observed.

The isotopic tracer results and the concurrency of the appearance of CO_2 and H_2 suggest that reaction 2 proceeds through a formate intermediate. The importance of the formate intermediate can be appreciated in terms of the following steps.

$$C^{18}O_s + {}^{16}OH_s \rightarrow \begin{matrix} & & C^{16}O_s + {}^{18}OH_s \\ & \nearrow & \\ HC^{16}O^{18}O_s & & \\ & \searrow & \\ & & C^{16}O^{18}O + \tfrac{1}{2}H_2 \end{matrix} \quad (3)$$

$$C^{18}O_s + {}^{18}OH_s \rightleftarrows HC^{18}O_s^{18} \rightarrow C^{18}O_2 + \tfrac{1}{2}H_2 \quad (4)$$

$$C^{16}O_s + {}^{16}OH_s \rightleftarrows HC^{16}O^{16}O_s \rightarrow C^{16}O_2 + \tfrac{1}{2}H_2 \quad (5)$$

Consistent with such a scheme, Figs. 6 and 7 indicate that the formation of $C^{18}O^{16}O$ is roughly twice that of either $C^{18}O_2$ or $C^{16}O_2$. The predominance of $C^{16}O_2$ in Fig. 8 is probably due to a rapid isotopic scrambling of $C^{18}O^{16}O$ and $C^{18}O_2$ with ^{16}OH groups present on the promoter. Such a process would be expected to proceed through either carbonate or bicarbonate groups. The infrared spectra presented in Fig. 2 clearly show carbonate species to be present on lanthana-promoted Rh/SiO_2.

Since the maximum temperature for CO_2 formation shifts downscale as the level of lanthana promotion increases, it is evident that OH groups associated with the promoter react more readily with adsorbed CO than OH groups associated with SiO_2. While the formate groups were not observed following CO chemisorption at 313 K, a well-defined formate band at 1580 cm^{-1} is generated during the exposure of lanthana-promoted Rh/SiO_2 to H_2 and CO at 530 K (*28*).

The mechanism by which lanthana promotion effects the disproportionation of CO, reaction 1, is more difficult to assess. One possibility is that the dissociation of CO, the first step in the processes, is facilitated by the interaction of lanthana cations with the oxygen end of CO molecules adsorbed along the perimeter of LaO_x patches. Such an interpretation would be consistent with the appearance of the CO band at 1725 cm^{-1}. Further support to the idea that lanthana cations assist in CO dissociation is provided by the TPSR results.

TPSR

Figure 9 clearly shows that chemisorbed CO is much more readily hydrogenated on lanthana-promoted Rh/SiO_2 than on unpromoted Rh/SiO_2. This trend is identical to that observed by Rieck and Bell (*33*) in their study of Pd/SiO_2 and Pd/SiO_2 promoted with rare-earth oxides. The possible reasons for the increased CO hydrogenation activity will be discussed in Part II of this study (*28*).

CO adsorption at 673 K on Rh/SiO_2 and lanthana-promoted Rh/SiO_2 results in the production of reactive surface carbon, which is readily hydrogenated at 293 K (see Fig. 10). As mentioned earlier, the quantity of reactive carbon formed, relative to the CO chemisorption capacity of the catalyst, is higher on the lanthana-promoted catalysts. These results indicate that the lantha-

num promoter assists in the dissociation of CO. Such an interpretation is consistent with the CO TPD results, which show that the amount of carbon formed by CO disproportionation, relative to the CO chemisorption capacity of each catalyst, increases with lanthana content.

It is interesting to note that the increase in the CO dissociation activity when Rh/SiO_2 is promoted with lanthana is consistent with the identification by infrared spectroscopy of a form of CO that absorbs at 1725 cm^{-1} and has a weakened C–O bond (Fig. 1). CO dissociation may occur more readily from this species than from CO on unmodified adsorption sites. The concentration of this species increases with lanthana content, from $La(0.5)/Rh/SiO_2$ to $La(5)/Rh/SiO_2$, as the results in Fig. 2 show. This observation is consistent with the TPSR and CO TPD results, which show that the quantity of surface carbon formed, relative to the CO chemisorption capacity of the catalyst, is higher for $La(5)/Rh/SiO_2$ than for $La(0.5)/Rh/SiO_2$.

SUMMARY AND CONCLUSIONS

Lanthana promotion of a Rh/SiO_2 catalyst has no effect on Rh particle size but results in an increasing coverage of the surface of the Rh crystallites with LaO_x moieties. With increasing level of lanthana promotion the capacity of the catalyst for CO chemisorption declines. A decline is also observed in the H_2 adsorption capacity, but it is smaller than that observed for CO because unlike CO, part of the H_2 adsorbed on the exposed Rh sites spills over onto the LaO_x patches.

Infrared spectra of CO adsorbed on lanthana-promoted Rh/SiO_2 exhibit bands characteristic of linearly and bridge-bonded CO present on Rh sites. Bands are also seen for carbonate groups associated with LaO_x islands. An additional band observed at 1725 cm^{-1} is attributed to CO adsorbed on surface Rh atoms near the edge of LaO_x islands, such that the oxygen end of the CO molecule interacts with lanthanum cations.

TPSR experiments show that adsorbed CO is more readily hydrogenated on lanthana-promoted Rh/SiO_2 than the unpromoted catalyst, in agreement with the higher steady-state CO hydrogenation activity observed for lanthana-promoted catalyst, increases with LaO_x content. These results indicate that lanthanum promotion assists in the dissociation of chemisorbed CO.

ACKNOWLEDGMENT

This work was supported by the Division of Chemical Sciences, Office of Basic Energy Sciences, U.S. Department of Energy, under Contract DE-AC03-76SF00098.

REFERENCES

1. Ichikawa, M., *Bull. Chem. Soc. Jpn.* **51,** 2273 (1978).
2. Orita, H., Naito, S., and Tamaru, K., *J. Catal.* **90,** 183 (1984).
3. Kip, B. J., Dirne, F. W. A., van Grondelle, J., and Prins, R., *ACS Symp., Div. Petr. Chem.* **31,** 163 (1986).
4. Arakawa, H., Takeuchi, K., Matsuzaki, T., and Sugi, Y., *Chem. Lett.*, p. 1607 (1984).
5. van't Blik, H. F. J., Vis, J. C., Huizinga, T., and Prins, R., *Appl. Catal.* **19,** 405 (1985).
6. Underwood, R. P., and Bell, A. T., *J. Catal.*, in press.
7. Ichikawa, M., and Shikakura, K., Proc. 7th Int. Congr. Catal., Tokyo, Part B, p. 925 (1980).
8. Katzer, J. R., Sleight, A. W., Gajardo, P., Michel, J. B., Gleason, E. F., and McMillan, S., *Faraday Discuss. Chem. Soc.* **72,** 121 (1981).
9. Solymosi, F., Tombacz, I., and Koszta, J., *J. Catal.* **95,** 578 (1985).
10. v.d. Lee, G., Schuller, B., Post, H., Favre, T. L. F., and Ponec, V., *J. Catal.* **98,** 522 (1986).
11. Gilhooley, K., Jackson, S. D., and Rigby, S., *Appl. Catal.* **21,** 349 (1986).
12. Kowalski, J., v.d. Lee, G., and Ponec, V., *Appl. Catal.* **19,** 423 (1985).
13. Kuznetsov, V. L., Romanenko, A. V., Mudrakovskii, I. L., Matikhin, V. M., Schmachkov, V. A., and Yermakov, Yu. I., Proc. 8th Int. Congr. Catal., Berlin **5,** 3 (1984).
14. Underwood, R. P., and Bell, A. T., *Appl. Catal.* **21,** 157 (1986).
15. Ellgen, P. C., Bartley, W. J., Bhasin, M. M., and Wilson, T. P., *Adv. Chem. Ser.* **178,** 147 (1979).
16. van den Berg, F. G. A., Glezer, J. H. E., and Sachtler, W. M. H., *J. Catal.* **93,** 340 (1985).

17. Sudhakar, C., Bhore, N., Bischoff, K. B., Manogue, W. H., and Mills, G. A., *ACS Symp., Div. Petr. Chem.* **31,** 133 (1986).
18. Arakawa, H., Fukushima, T., Ichikawa, M., Natsushita, S., Takeuchi, K., Matsuzaki, T., and Sugi, Y., *Chem. Lett.*, p. 881 (1985).
19. Naito, S., Kagami, S., Yoshioka, H., Kobori, Y., Onishi, T., and Tamaru, K., *Proc. Symp. Heterog. Catal., Dalian, China* (1982).
20. Kagami, S., Naito, S., Kikuzono, Y., and Tamaru, K., *J. Chem. Soc. Chem. Commun.*, p. 256 (1983).
21. Orita, H., Naito, S., and Tamaru, K., *Chem. Lett.*, p. 1161 (1983).
22. Chuang, S. C., Goodwin, J. G., and Wender, I., *J. Catal.* **95,** 435 (1985).
23. Ichikawa, M., Sekizawa, K., and Shikakura, K., *J. Mol. Catal.* **11,** 167 (1981).
24. Ichikawa, M., Shikakura, K., and Kawaii, M., *Proc. Symp. Heterog. Catal., Dalian, China* (1982).
25. Ichikawa, M., Fukushima, T., and Shikakura, K., Proc. 8th Int. Congr. Catal., Berlin **2,** 69 (1984).
26. Fukushima, T., Ichikawa, M., Matsushita, S., Tanaka, K., and Saito, T., *J. Chem. Soc. Chem. Commun.*, p. 1209 (1985).
27. Kiennemann, A., Breault, R., Hindermann, J. P., and Laurin, M., *Faraday Symp. Chem. Soc.* **21,** 14 (1986).
28. Underwood, R. P., and Bell, A. T., *J. Catal.*, in press.
29. Hicks, R. F., Kellner, C. S., Savatsky, B. J., Hecker, W. C., and Bell, A. T., *J. Catal.* **71,** 216 (1981).
30. Rieck, J. S., and Bell, A. T., *J. Catal.* **96,** 99 (1985).
31. Primet, M., *J. Catal.* **88,** 273 (1984).
32. Tascon, J. M. D., Oliven, A. M. O., Tejuca, L. G., and Bell, A. T., *J. Phys. Chem.* **90,** 791 (1986).
33. Rieck, J. S., and Bell, A. T., *J. Catal.* **99,** 278 (1986).
34. Hicks, R. F., Yen, Q.-J., and Bell, A. T., *J. Catal.* **89,** 498 (1984).
35. Rosynek, M. P., and Magnuson, D. T., *J. Catal.* **48,** 417 (1977).
36. Busca, G., and Lorenzelli, V., *Mater. Chem.* **7,** 89 (1982).
37. Shriver, D. F., *ACS Symp. Ser.* **152,** 1 (1981).
38. Horwitz, C. P., and Shriver, D. F., *Adv. Organomet. Chem.* **23,** 219 (1984).
39. Ichikawa, M., and Fukushima, T., *J. Phys. Chem.* **89,** 1564 (1985).
40. Jackson, S. D., *J. Chem. Soc. Faraday Trans. I* **81,** 2225 (1985).